08,03

Creation of optically addressable spin centers in hexagonal boron nitride by proton irradiation

© F.F. Murzakhanov[1], I.E. Mumdzhi[1], G.V. Mamin[1], R.V. Yusupov[1], V.Yu. Davydov[2], A.N. Smirnov[2], M.V. Muzafarova[2], S.S. Nagalyuk[2], V.A. Soltamov[1]

[1] Institute of Physics, Kazan Federal University, Kazan, Russia
[2] Ioffe Institute, St. Petersburg, Russia

E-mail: marina.muzafarova@mail.ioffe.ru, murzakhanov.fadis@yandex.ru

Received April 13, 2022
Revised April 13, 2022
Accepted April 19, 2022

The possibility of creating defects with spin-dependent fluorescence in a Van der Waals material, hexagonal boron nitride (hBN), by irradiating the latter with high-energy protons ($E_P = 15$ MeV) has been studied. Using micro-photoluminescence and electron paramagnetic resonance methods it was shown that such irradiation leads to the creation of boron vacancies in the negative charge state (V_B^--centers). The ground spin triplet ($S = 1$) state of these defects demonstrates an optically induced inverse population.

Keywords: electron paramagnetic resonance, micro-photoluminescence, hexagonal boron nitride, boron vacancy.

DOI: 10.21883/PSS.2022.08.54624.349

1. Introduction

One of the main criteria of applicability of optically active defects in wide-band-gap semiconductors for the development of quantum technologies is the defect's having of a path of spin-dependent recombination under the action of optical pumping, which results in predominant occupation of one of the spin sublevels of the defect [1]. This property allows for converting the defect spin state into an optical quantum by scanning the microwave frequency — excitation of transitions of electron paramagnetic resonance (EPR) between electron spin sublevels, making it possible to read the spin by means of an optically detected magnetic resonance (ODMR) [1–3]. The most well-studied defects of this type include a negatively charged nitrogen-vacancy defect in a diamond and vacancy defects in silicon carbide [1,2,4–7]. Using optically-generated high-spin states of such defects, we have managed to suggest and implement quantum sensors of a high spatial resolution [5,8,9], quantum networks [10], masers active at room temperature [11,12]. However, both the diamond and silicon carbide, being made up of sp^3-hybridized atoms, are 3D crystalline matrices.

A totally different matrix for optically active defects is a broad class of the so-called van der Waals (vdW) materials, in particular, hexagonal boron nitride (hBN), which, thanks to a super-wide band gap ($E_g \approx 6$ eV) [13], can contain defects active in a range from UV to IR [14,15]. sp^2-hybridization inherent in hexagonal boron nitride leads to the formation of two-dimensional layers where atoms are linked by strong planar-trigonal covalent σ bonds, while the 2D-layers themselves are linked by weak van der Waals forces. Breaking of the weak vdW interaction allows for the making of materials being the limit condensed state of matter — a monoatomic layer whose unique properties are largely due to the planar-trigonal structure [16].

Spin and optical properties of defects in a hBN matrix are being actively studied at present [13] in view of the recently demonstrated possibility to use them as sources of single photons [17–19], qubits [20,21], quantum sensors of magnetic fields, temperature and pressure [22,23]. It has been recently shown that luminescence of a number of centers in hBN is spin-dependent, which allows for recording of the corresponding ODMR signals [24–27]. It should be noted, however, that the nature and microscopic structure of only one optically active defect has been unambiguously established at present. This defect is a negatively charged boron vacancy (V_B^--center), being in a regular environment of three nitrogen atoms (Fig. 1, *a*) [21,24], spin and optical properties of which are briefly outlined in Fig. 1, *b* in compliance with the previously obtained results [21,24]. Further study of the properties of these defects requires a tool for their reproducible and controllable creation in a boron nitride matrix.

In the present paper we show that such a tool is hBN irradiation with high-energy protons. It should be noted that the possibility to generate such defects by irradiating boron nitride with high-energy neutrons and electrons [24,29], nitrogen ions [30], as well as by means of femtosecond laser pulses has been previously studied [31].

2. Experimental part

Commercially available single crystals of hexagonal boron nitride (manufactured by hq Graphene) were irradiated with

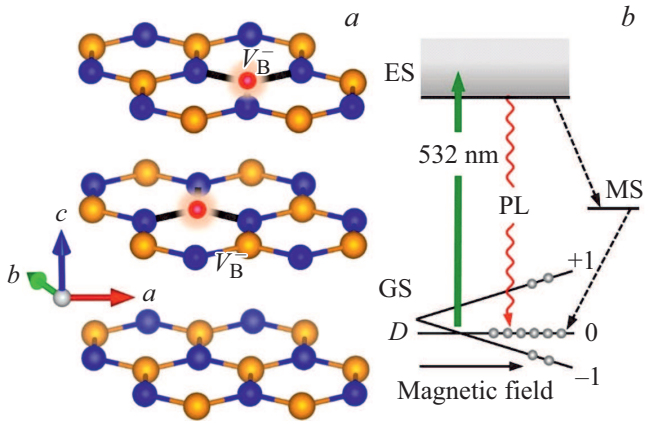

Figure 1. *a* — hBN structure with boron vacancies (shown as red balls). The blue color shows the nitrogen atoms, the yellow color — boron atoms. *a, b, c* are directions of the crystalline lattice base vectors, axis *c* is a hexagonal axis perpendicular to the base 2D BN-planes. The black continuous lines show the broken bonds. *b* — the energy diagram of the levels of the optical pumping cycle for spin sublevel $m_s = 0$ of the ground triplet state ($S = 1$) of V_B^--centers. Splitting of spin sublevels in a zero magnetic field is designated as *D*. The ground state is split by an external magnetic field. Optical excitation with $\lambda = 532$ nm (a solid arrow) leads to electron transitions from the ground state (GS) to the excited state (ES) and by way of optical recombination (PL, red wavy line) back to the ground state without electron spin change. Since the system contains levels of the metastable state (MS), spin-dependent recombination takes place (marked with dashed arrows) and leads to the predominant population with $m_s = 0$.

protons in an isochronous cyclotron with the following parameters: proton energy $E_P = 15$ MeV, total irradiation dose $1 \cdot 10^{16}$ cm^{-2}. The range of sample temperatures under proton irradiation was within 20−100°C. After irradiation, the hBN samples were studied by micro-photoluminescence (μ-PL) and electron paramagnetic resonance (EPR) in order to reveal defects generated by the radiation action. The μ-PL experiments were conducted using a T64000 spectrometer (Horiba Jobin-Yvon, Lille, France) equipped with a confocal microscope and a silicon CCD matrix cooled to the liquid nitrogen temperature. Luminescence was excited using the $\lambda = 532$ nm line (2.3308 eV) of the Nd:YAG-laser. The laser beam was focused on the sample surface using a Leica PL FLUOTAR 50× lens (NA = 0.55) to a spot with the diameter of $\sim 2\,\mu$m. Luminescence spectra were recorded using a 600 grooves/mm diffraction grating. EPR studies were conducted using a commercial EPR spectrometer manufactured by Bruker Elexsys 680 in the W-range (frequency 94 GHz). Sample cooling was provided using an Oxford Instruments ESR-9 continuous-flow helium cryostat (Abingdon, Oxfordshire, UK).

3. Results and discussion

Fig. 2, *a* shows the low-temperature photoluminescence spectrum of the hBN sample after proton irradiation. The observed wide band in the near IR-range corresponds to the spectral band of boron vacancies in a negative charge state, as has been demonstrated previously in several papers using the ODMR method [20,24,28]. It should be noted that the above-mentioned peculiarities were not observed in the hBN sample before proton irradiation.

The weakly intensive peak in the PL spectrum with the maximum at the wavelength of $\lambda = 772.4$ nm, shown in the inset in Fig. 2, *a* in an enlarged scale, corresponds to the zero phonon line of V_B^--centers, as has been demonstrated previously in [32,33]. In particular, the maximum of this zero-phonon line in [33] was found to be equal to $\lambda = 773 \pm 2$ nm. It should be noted that the hBN sample did not have the above-mentioned spectral singularities prior to proton irradiation, as can be seen from the init. spectrum in Fig. 2, *a*. A distinctive feature of V_B^--centers is their active PL at room temperature as well, as shown in Fig. 2, *b*. Thus, we have shown the presence of all optical characteristics which confirm the successful creation of V_B^--centers using proton irradiation.

The ground state of V_B^--centers exclusive of hyperfine interactions with cores of nitrogen and boron sublattices is described by a spin Hamiltonian (1), which includes a Zeeman term, and terms describing the splitting of spin sublevels in a zero magnetic field, presence of which causes the formation of a fine structure in the EPR spectrum due to partial withdrawal of spin degeneracy

$$H = g\mu_B \mathbf{B} \cdot \mathbf{S} + D(S_z^2 - 2/3) + E(S_x^2 - S_y^2), \qquad (1)$$

where $\mathbf{S}$ — electron spin operator, μ_B — Bohr magneton, g — factor of spectroscopic splitting, $\mathbf{B}$ — constant mag-

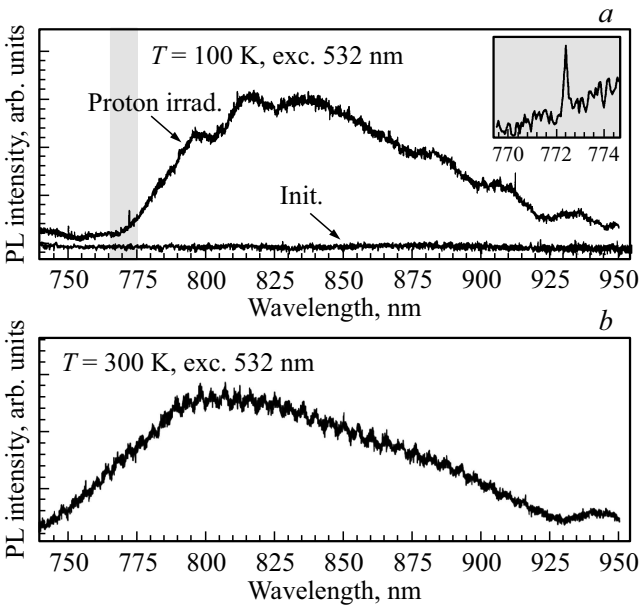

Figure 2. *a* — photoluminescence of the hBN sample recorded before (init.) and after proton irradiation at $T = 100$ K, excitation by a Nd:YAG laser line $\lambda = 532$ nm. The right inset shows the zero-phonon line of the V_B^--centers (the maximum on the wavelength of $\lambda = 772.4$ nm). *b* — PL spectrum of the proton-irradiated hBN sample, recorded at $T = 300$ K.

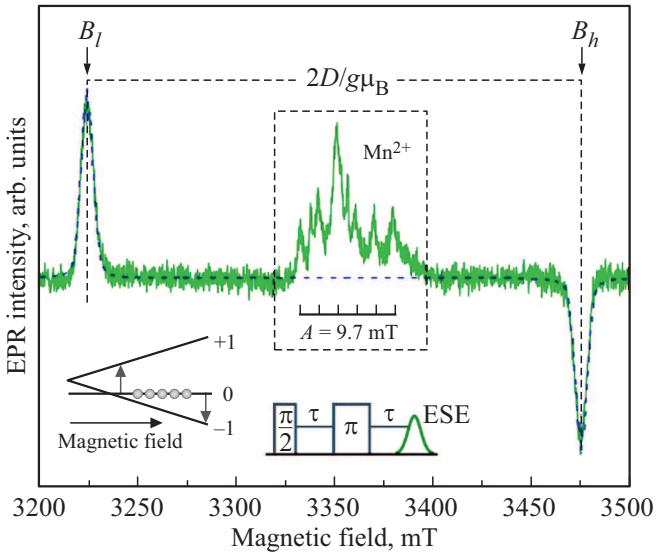

Figure 3. EPR spectrum (green color) of the proton-irradiated hBN sample, recorded in the mode of electron spin echo at 50 K and laser excitation with $\lambda = 532$ nm. The EPR spectrum simulation is also shown (dashed line) with account of fine structure manifestation and inversion of triplet center population with predominant population of the spin sublevel $m_s = 0$. The resonant magnetic fields are marked as B_l and B_h in compliance with the triplet sublevel diagram shown in the left-hand inset. The lower inset shows the Hahn pulse sequence used for detection of electron spin echo. The frame shows a spurious signal from the Mn^{2+} centers in the resonator, with a typical hyperfine structure $A = 9.7$ mT.

netic field; D and E — parameters of fine structure (zero splitting); S_z, S_x and S_y — spin operators of triplet center projection, the z axis is collinear to the hexagonal c axis.

Fig. 3 shows the EPR spectrum recorded in the mode of primary electron spin echo in the proton-irradiated hBN sample. The hBN sample was positioned so that its hexagonal c axis was parallel to the vector of constant magnetic field **B** ($B \parallel c$, $\theta = 0°$). The EPR spectrum was recorded at 50 K using optical excitation with $\lambda = 532$ nm. The doublet of the lines in the magnetic fields marked in Fig. 3 as B_l and B_h reflects the splitting present in the zero magnetic field (D), caused chiefly by a spin-spin interaction. Thus, this pair of lines, spaced apart at the distance of $\Delta B = 2D/g\mu_B = 252.1$ mT from each other, corresponds to the permitted transitions of EPR $\Delta m_s = \pm 1$ between the triplet spin sublevels, as shown schematically in the inset in Fig. 3. The EPR spectrum was simulated (see the dashed line in Fig. 3) using a spin Hamiltonian (1) and parameters $g = 2.0035$, $D = 3530$ MHz and $E = 50$ MHz, which correspond to the spectroscopic parameters of the V_B^--centers [24]. Thanks to a metastable intermediate level present in the spin-dependent path of excitation-recombination (see Fig. 1, *b*) of paramagnetic centers, laser excitation causes an intense repopulation of all three spin levels. Thereat, the thermodynamic Boltzmann equilibrium is disrupted, where the non-magnetic level $m_s = 0$ becomes the most populated. Due to this effect, the low-field component B_l of the fine structure in the EPR structure manifests itself as an absorption line, while the high-field component B_h manifests itself as radiation (an inverted signal). The region of $g = 2.003$ (center of gravity of the EPR spectrum of the boron vacancy) contains a signal having a structure of 6 equidistant lines with splitting ≈ 97 G. This typical structure pertains to an isotropic hyperfine interaction of Mn^{2+} (marked with a frame in Fig. 3). These manganese ions do not pertain to the hBN sample, but are resonator signals which do not respond to the laser irradiation.

4. Conclusion

The photoluminescence and electron paramagnetic resonance methods have shown the suitability of proton irradiation for the creation of V_B^--centers in hexagonal boron nitride. Taking into account the strong interest in the study of spin and optical properties of V_B^--centers [21–24,28], these results are extremely topical at present. A distinctive feature of proton irradiation is a high level of control of spatial positioning of defects in the crystalline matrix [36,37], which is attained by proton beam focusing to a spot up to 100 nm^2 in diameter. The latter can be used to create both ensembles and single defects with submicron spatial positioning. On the other hand, an important characteristic of the used irradiation is the fact that H^+ ions are lightweight and make the minimum contribution to secondary radiation-induced defect formation and are characterized by the minimum Bragg peak, making it possible to avoid regions of significant clustering of defects which adversely affect the spin and optical properties of defects [36,37].

Funding

The work was supported by a grant of the Russian Science Foundation No. 20-72-10068.

Conflict of interest

The authors declare that they have no conflict of interest.

References

[1] D. Awschalom, R. Hanson, J. Wrachtrup, B.B. Zhou. Nature Photon. **12**, 516 (2018).
[2] P.G. Baranov, H.J. von Bardeleben, F. Jelezko, J. Wrachtrup. Magnetic Resonance of Semiconductors and Their Nanostructures: Basic and Advanced Applications. Springer Series in Material Science. Springer, Heidelberg (2017). 525 p.
[3] D. Suter. Magn. Res. **1**, 115 (2020).
[4] M.W. Doherty, N.B. Manson, P. Delaney, F. Jelezko, J. Wrachtrup, L.C.L. Hollenberg. Phys. Rep. **528**, *1*, 1 (2013).
[5] C.-L. Degen, F. Reinhard, P. Cappellaro. Rev. Mod. Phys. **89**, 035002 (2017).

[6] G.V. Astakhov, D. Simin, V. Dyakonov, B.V. Yavkin, S.B. Orlinskii, I.I. Proskuryakov, A.N. Anisimov, V.A. Soltamov, P.G. Baranov. Appl. Magn. Res. **47**, 793 (2016).
[7] T. Biktagirov, W. Gero Schmidt, U. Gerstmann, B. Yavkin, S. Orlinskii, P. Baranov, V. Dyakonov, V. Soltamov. Phys. Rev. B **98**, 195204 (2018).
[8] N. Aslam, M. Pfender, P. Neumann, R. Reuter, A. Zappe, F.F. de Oliveira, A. Denisenko, H. Sumiya, Sh. Onoda, J. Isoya, J. Wrachtrup. Science **357**, *6346*, 67 (2017).
[9] D. Simin, V.A. Soltamov, A.V. Poshakinskiy, A.N. Anisimov, R.A. Babunts, D.O. Tolmachev, E.N. Mokhov, M. Trupke, S.A. Tarasenko, A. Sperlich, P.G. Baranov, V. Dyakonov, G.V. Astakhov. Phys. Rev. X **6**, 031014 (2018).
[10] P.C. Humphreys, N. Kalb, J.P.J. Morits, R.N. Schouten, R.F.L. Vermeulen, D.J. Twitchen, M. Markham, R. Hanson. Nature **558**, 268 (2018).
[11] H. Kraus, V.A. Soltamov, D. Riedel, S. Vath, F. Fuchs, A. Sperlich, P.G. Baranov, V. Dyakonov, G.V. Astakhov. Nature Phys. **10**, 157 (2014).
[12] J.D. Breeze, E. Salvadori, J. Sathian, N.McN. Alford, Ch.W.M. Kay. Nature **555**, 493 (2018).
[13] G. Cassabois, P. Valvin, B. Gil. Nature Photon. **10**, 262 (2016).
[14] J.D. Caldwell, I. Aharonovich, G. Cassabois, J.H. Edgar, B. Gil, D.N. Basov. Nature Rev. Mater. **4**, 552 (2019).
[15] A. Dietrich, M. Bürk, E.S. Steiger, L. Antoniuk, T.T. Tran, M. Nguyen, I. Aharonovich, F. Jelezko, A. Kubanek. Phys. Rev. B **98**, 081414(R) (2018).
[16] A.K. Geim, I.V. Grigorieva. Nature **499**, 7459 (2013).
[17] T.T. Tran, K. Bray, J. Ford, Michael, M. Toth, I. Aharonovich. Nature Nanotech. **11**, 37 (2015).
[18] L.J. Martínez, T. Pelini, V. Waselowski, J.R. Maze, B. Gil, G. Cassabois, V. Jacques. Phys. Rev. B **94**, 121405(R) (2016).
[19] X. Xu, Z.O. Martin, D. Sychev, A.S. Lagutchev, Y.P. Chen, T. Taniguchi, K. Watanabe, V.M. Shalaev, A. Boltasseva. Nano Lett. **21**, *19*, 8182 (2021).
[20] A. Gottscholl, M. Diez, V. Soltamov, C. Kasper, A. Sperlich, M. Kianinia, C. Bradac, I. Aharonovich, V. Dyakonov. Sci. Adv. **7**, 14 (2021).
[21] V. Ivády, G. Barcza, G. Thiering, S. Li, H. Hamdi, J.-P. Chou, O. Legeza, A. Gali. npj Comput. Mater. **6**, 41 (2020).
[22] A. Gottscholl, M. Diez, V. Soltamov, C. Kasper, D. Krauße, A. Sperlich, M. Kianinia, C. Bradac, I. Aharonovich, V. Dyakonov. Nature Commun. **12**, 4480 (2021).
[23] J.-P. Tetienne. Nature Phys. **17**, 1074 (2021).
[24] A. Gottscholl, M. Kianinia, V. Soltamov, S. Orlinskii, G. Mamin, C. Bradac, C. Kasper, K. Krambrock, A. Sperlich, M. Toth, I. Aharonovich, V. Dyakonov. Nature Mater. **19**, 540 (2020).
[25] N. Chejanovsky, A. Mukherjee, J. Geng, Yu-C. Chen, Y. Kim, A. Denisenko, A. Finkler, T. Taniguchi, K. Watanabe, D.B.R. Dasari, P. Auburger, A. Gali, J.H. Smet, J. Wrachtrup. Nature Mater. **20**, 1079 (2021).
[26] H.L. Stern, J. Jarman, Q. Gu, S.E. Barker, N. Mendelson, D. Chugh, S. Schott, H.H. Tan, H. Sirringhaus, I. Aharonovich, M. Atatüre. Nature Commun. **13**, 618 (2022).
[27] N.-J. Guo, Y.-Ze Yang, X.-D. Zeng, S. Yu, Yu Meng, Z.-P. Li, Z.-A. Wang, L.-K. Xie, J.-S. Xu, J.-F. Wang, Q. Li, W. Liu, Y.-T. Wang, J.-S. Tang, C.-F. Li, G.-C. Guo. arXiv:2112.06191 (2021).
[28] S. Baber, R. Nicholas, E. Malein, P. Khatri, P.S. Keatley, Shi Guo, F. Withers, A.J. Ramsay, I.J. Luxmoore. Nano Lett. **22**, *1*, 461 (2022).
[29] F.F. Murzakhanov, B.V. Yavkin, G.V. Mamin, S.B. Orlinskii, I.E. Mumdzhi, I.N. Gracheva, B.F. Gabbasov, A.N. Smirnov, V.Yu. Davydov, V.A. Soltamov. Nanomaterials **11**, 1373 (2021).
[30] N.-J. Guo, W. Liu, Z.-P. Li, Y.-Z. Yang, S. Yu, Y. Meng, Z.-A. Wang, X.-D. Zeng, F.-F. Yan, Q. Li, J.-F. Wang, J.-S. Xu, Y.-T. Wang, J.-S. Tang, C.-F. Li, G.-C. Guo. ACS Omega **7**, *2*, 1733 (2022).
[31] X. Gao, S. Pandey, M. Kianinia, J. Ahn, P. Ju, I. Aharonovich, N. Shivaram, T. Li. ACS Photonics **8**, *4*, 994 (2021).
[32] J.E. Fröch, L. Spencer, M. Kianinia, D. Toton-jian, M. Nguyen, V. Dyakonov, M. Toth, S. Kim, I. Aharonovich. Nano Lett. **21**, *15*, 6549 (2021).
[33] C. Qian, V. Villafañe, M. Schalk, G.V. Astakhov, U. Kentsch, M. Helm, P. Soubelet, N.P. Wilson, R. Rizzato, S. Mohr, A.W. Holleitner, D.B. Bucher, A.V. Stier, J.J. Finley. arXiv:2202.10980 (2022).
[34] F. Watt, M.B.H. Breese, A.A. Bettiol, J.A. van Kan. Mater. Today **10**, *6*, 20 (2007).
[35] H. Kraus, D. Simin, C. Kasper, Y. Suda, S. Kawabata, W. Kada, T. Honda, Y. Hijikata, T. Ohshima, V. Dyakonov, G.V. Astakhov. Nano Lett. **17**, *5*, 2865 (2017).
[36] T.B. Biktagirov, A.N. Smirnov, V.Yu. Davydov, M.W. Doherty, A. Alkauskas, B.C. Gibson, V.A. Soltamov. Phys. Rev. B **96**, 075205 (2017).
[37] F.F. Murzakhanov, G.V. Mamin, S.B. Orlinskii, U. Gerstmann, W.G. Schmidt, T. Biktagirov, I. Aharonovich, A. Gottscholl, A. Sperlich, V. Dyakonov, V.A. Soltamov. arXiv:2112.10628 (2021).